

Chapter

FAD-Linked Autofluorescence and Chemically-Evoked Zinc Changes at Hippocampal Mossy Fiber-CA3 Synapses

*Fatima M.C. Bastos, Carlos M. Matias, Ines O. Lopes,
João P. Vieira, Rosa M. Santos, Luis M. Rosario,
Rosa M. Quinta-Ferreira and Maria Emilia Quinta-Ferreira*

Abstract

Glutamatergic vesicles in hippocampal mossy fiber presynaptic boutons release zinc, which plays a modulatory role in synaptic activity and LTP. In this work, a fluorescence microscopy technique and the fluorescent probe for cytosolic zinc, Newport Green (NG), were applied, in a combined study of autofluorescence and zinc changes at the hippocampal mossy fiber-CA3 synaptic system. In particular, the dynamics of flavoprotein (FAD) autofluorescence signals, was compared to that of postsynaptic zinc signals, elicited both by high K^+ (20 mM) and by tetraethylammonium (TEA, 25 mM). The real zinc signals were obtained subtracting autofluorescence values, from corresponding total NG-fluorescence data. Both autofluorescence and zinc-related fluorescence were raised by high K^+ . In contrast, the same signals were reduced during TEA exposure. It is suggested that the initial outburst of TEA-evoked zinc release might activate ATP-sensitive K^+ (K_{ATP}) channels, as part of a safeguard mechanism against excessive glutamatergic action. This would cause sustained inhibition of zinc signals and a more reduced mitochondrial state. In favor of the “ K_{ATP} channel hypothesis”, the K_{ATP} channel blocker tolbutamide (250 μ M) nearly suppressed the TEA-evoked fluorescence changes. It is concluded that recording autofluorescence from brain slices is essential for the accurate assessment of zinc signals and actions.

Keywords: autofluorescence, Newport Green, K_{ATP} channels, TEA, tolbutamide, hippocampal slices

1. Introduction

Glutamatergic vesicles in hippocampal mossy fiber presynaptic boutons sequester and actively release zinc together with glutamate [1, 2]. Once released, zinc diffuses in the synaptic cleft and binds to specific sites mainly in the postsynaptic CA3 neuronal membrane, crossing it via calcium-permeable glutamate receptors and voltage-dependent calcium channels (VDCCs) [3–8]. Thus, zinc plays significant modulatory roles in synaptic activity and possibly also in long-term potentiation

(LTP) [2, 9–12]. A negative feedback action at presynaptic sites seems also to occur, when released zinc activates the ATP-sensitive K^+ (K_{ATP}) channels [13, 14], besides inhibiting VDCCs [15, 16] on the boutons. These processes are thought to protect synapses from excessive neurotransmitter release and, consequently, too much postsynaptic activity.

In previous studies, performed using intracellularly trapped fluorescent dyes as zinc probes, it has been shown that single and tetanic stimulation of mossy fibers evoke zinc release and postsynaptic intracellular zinc rises [17–19]. It has also been reported that the application of high external potassium concentrations elicits a strong depolarization in the cells [20, 21], as well as postsynaptic zinc enhancements [22]. However, the application of intense tetanic stimulation caused a depression of zinc and glutamate release, which was reduced by the application of the K_{ATP} channel blocker tolbutamide [14]. Furthermore, in the presence of the potassium channel blocker tetraethylammonium (TEA), which induces a weaker depolarization in the mossy fiber region [23], the zinc signals were reversibly depressed being this depression also reduced by tolbutamide [24]. Since the depolarizing effect of KCl is stronger than that of TEA, it is expected that the increase of the synaptic activity will be more intense in the presence of KCl. The postsynaptic actions of zinc may not be limited to the membrane or the cytosol, as there is evidence that this cation is taken up by cell organelles including the endoplasmic reticulum and mitochondria [4, 25, 26]. Recording zinc probe fluorescence from slices is not devoid of artifacts. A potential problem is the tissue autofluorescence, which depends on the excitation wavelengths, which may arise from both NAD(P)H (near-UV) and flavoprotein-bound FAD (visible) [27–29]. In the present experiments, which were performed using the fluorescent zinc indicator Newport Green (NG), the prevailing contributor to autofluorescence was the FAD-linked fluorescence, since NG was excited with visible light. The redox couple FAD/FADH₂ operates in the citric acid cycle and respiratory chain, and this autofluorescence component might originate mostly, if not exclusively from mitochondria [30–32]. Furthermore, dehydrogenases are calcium-sensitive [33], suggesting that FAD-linked autofluorescence might change following stimulation of hippocampal mossy fibers. Thus, an important objective of this study was to determine whether mossy fiber autofluorescence might affect the zinc signals and, if so, to extract the real dynamics of the zinc signals from the total fluorescence recordings. Autofluorescence of mitochondrial origin reflects the metabolic activity of the cells. Therefore, carrying out parallel autofluorescence recordings offers the possibility of correlating the postsynaptic zinc dynamics of pyramidal CA3 neurons with changes in tissue metabolic activity.

2. Experimental procedures

All experiments were carried out in accordance with the Directive 2010/63/EU of the European Parliament and Council. In agreement with the Portuguese law, the animal care review committee is the *Direção-Geral de Alimentação e Veterinária* (DGAV). All efforts were made to minimize animal suffering and to use only the number of animals necessary to produce reliable scientific data.

The experiments were performed in the synaptic system mossy fibers-CA3 pyramidal cells, using the brain of pregnant Wistar rat females (16–18 weeks old), kindly provided by the CNC (Center for Neurosciences) laboratory (as stated in the acknowledgments). The hippocampal slices were prepared as previously described [22, 24]. Briefly, after cervical dislocation, the isolated brain was rapidly cooled (5–8°C) in oxygenated (95% O₂, 5% CO₂) artificial cerebrospinal fluid (ACSF), containing (in mM): NaCl 124; KCl 3.5; NaHCO₃ 24; NaH₂PO₄ 1.25; MgCl₂ 2; CaCl₂

2 and D-glucose 10, pH 7.4. Then, the hippocampus was separated and the slices (400 μm thick) were cut transversely and immersed in ACSF at room temperature. After a resting period of about 1 h, the slices were transferred to the experimental chamber and perfused with ACSF, at a rate of 1.5 to 2 ml/min, $T = 30\text{--}32^\circ\text{C}$.

Autofluorescence measurements were carried out in slices immersed in ACSF or in the medium of interest. For the detection of zinc changes, the slices were incubated during one hour in an ACSF solution containing 5 μM of the permeant form of the fluorescent zinc indicator Newport Green (NG). The preparation of the solution was performed as follows: 1 mg of NG was dissolved in 250 μl of DMSO and then 5 μl of this mixture (DMSO + NG) were diluted in 5 ml of ACSF containing 5 μl of pluronic acid F-127. The indicator NG has a moderate affinity for zinc ($K_d \sim 1 \mu\text{M}$) and a relatively low affinity for calcium ($K_d > 100 \text{ mM}$).

The fluorescence signals recorded from NG loaded slices contain an autofluorescence and a zinc-NG components. Having been realized that the first component varies both with time and with the perfusing medium, fluorescence signals from dye-free slices were recorded using similar experimental protocols as those applied in the NG containing slices. The real zinc signals were thus obtained from those measured from the indicator-loaded slices, after point-to-point subtraction of the intrinsic fluorescence records. Both types of records were normalized by the average of the baseline (first ten points) values prior to the mentioned subtraction, to avoid non-intrinsic and non-dye associated fluorescence. For the correction procedure, the following equations were used:

$$F_{A0} = \frac{\sum_{i=1}^{10} F_{Ai}}{10} \quad (1)$$

The corrected and normalized signals were represented as:

$$\frac{F_i}{F_0} = 1 + \left(\frac{F_{Ti}}{F_{T0}} - \frac{F_{Ai}}{F_{A0}} \right) \quad (2)$$

F_{A0} – basal autofluorescence; F_{Ai} – autofluorescence; F_{T0} – basal total fluorescence; F_{Ti} – total fluorescence; F_i – zinc fluorescence; F_0 – basal zinc fluorescence.

In order to study the role of zinc in autofluorescence changes evoked by chemical stimulation with KCl, the zinc chelator ethylenediaminetetraacetic acid disodium calcium salt (Ca-EDTA), (25 mM), was, in some experiments, added to the medium. The KCl solution consisted of ACSF but with 20 mM concentration of KCl. The tetraethylammonium (TEA) solution consisted of ACSF with higher concentrations of CaCl_2 and KCl, 10 mM and 5 mM, respectively, and with TEA at a concentration of 25 mM. The K_{ATP} channel blocker tolbutamide (250 μM) was directly applied to the perfusion medium, which was recirculated. All solutions were applied for periods of 30 min, except the KCl + Ca-EDTA solution that was perfused for 1 h.

The detection and measurement of zinc signals was performed using an experimental transfluorescence setup based on a microscope (Zeiss Axioskop), equipped with a halogen light source (12 V, 100 W). Excitation and emission wavelengths were selected by means of a narrowband filter (480 nm, BW 10 nm) and a high pass filter (> 500 nm), respectively. The capture of the transmitted light was done by a water immersion lens (40x, N.A. 0.75), being that light focused on a photodiode (Hamamatsu, 1 mm^2). Subsequently, the current of the photodiode was converted in an electrical signal by a current/voltage converter (I/V), with a feedback resistance of 1 G Ω . The signal was digitally processed by a 16 bit analog/digital converter

($f = 1.67$ Hz) and analyzed using the Signal Express™ software from National Instruments. The average value of each group of 100 consecutive points was used in order to illustrate the results.

All data are expressed as mean \pm SEM. The results of the statistical studies were obtained using the Mann–Whitney U test ($p < 0.05$).

In the experiments, the chemical products used were: NG, Pluronic acid F-127 (Life technologies, Carlsbad, CA); DMSO, TEA, Tolbutamide (Sigma-Aldrich, Sintra, PT).

3. Results

In this study, fluorescence changes evoked by the application of KCl and TEA media were measured both from non-incubated and from NG loaded slices. In most figures the first 10 min represent data from slices exposed to the ACSF solution, the next 30 min data evoked by the media of interest (KCl or TEA) and in the following 30 min ACSF was again perfused. Since the excitation wavelength used was 480 nm, the recorded fluorescence emission from dye-free slices is considered essentially autofluorescence, with flavoprotein origin. Taking into account the spectral characteristics of the intrinsic fluorescence of FAD and of zinc-bound NG, the fluorescence signals obtained from slices incubated in NG, using excitation light of 480 nm and recording above 500 nm, have two different components: autofluorescence and the fluorescence of the zinc-NG complex. The results of a group of experiments designed to extract the real zinc signal, as the difference between those two components, are shown in **Figure 1**.

The autofluorescence trace (**Figure 1a**) reveals that the KCl (20 mM) solution caused an increase of the signals, of $11 \pm 2\%$ in the period 35–40 min ($n = 4$). The total fluorescence signals (**Figure 1b**) were enhanced by $36 \pm 5\%$ above the basal values in the same period ($n = 3$). Thus, it can be observed that the zinc signals (**Figure 1c**), obtained as the total fluorescence minus the autofluorescence changes, reached a stable value having an amplitude of $27 \pm 3\%$ during the last 5 min in KCl. The autofluorescence changes continued to increase during the reperfusion of ACSF, reaching a maximum between 45 and 50 min after the beginning of the experiment, corresponding to an amplitude of $20 \pm 2\%$ above baseline. Afterwards they decreased again to $11 \pm 2\%$. The total fluorescence trace decreased less during washout, having an amplitude of $29 \pm 4\%$ during the last 5 min. The zinc signals decreased during the first 10 min of washout but were maintained in the remaining period at $16 \pm 4\%$ above baseline.

Unlike the behavior observed with KCl, both the autofluorescence and the total fluorescence signals were reduced in the presence of 25 mM TEA, recovering, upon its removal, to a value above the baseline (**Figure 2a** and **b**). The application of TEA caused a decline of the amplitude of the total signal (**Figure 2b**) by $17 \pm 3\%$ of control (35–40 min., $n = 8$). In these experiments, autofluorescence (**Figure 2a**) was responsible for almost half of the depression since the intrinsic signals decreased by $8 \pm 2\%$ (35–40 min, $n = 5$). Consequently, it can be concluded that the zinc signals (**Figure 2c**), obtained again as the difference between the traces in panels b and a, were reduced by $9 \pm 1\%$, in the same period.

The superimposed results of the autofluorescence and of the corresponding zinc signals are shown in **Figure 3**, for the experiments performed with KCl (**Figure 3a**) and TEA (**Figure 3b**). They reveal that the signals from the unincubated and the NG-treated slices have different time courses in the case of KCl, rising the autofluorescence transients more slowly than the zinc ones (**Figure 3a**). TEA causes roughly similar autofluorescence and zinc changes (**Figure 3b**). It should also be noticed that the KCl evoked zinc changes remained potentiated upon washout, while, following TEA removal the zinc signals recovered completely.

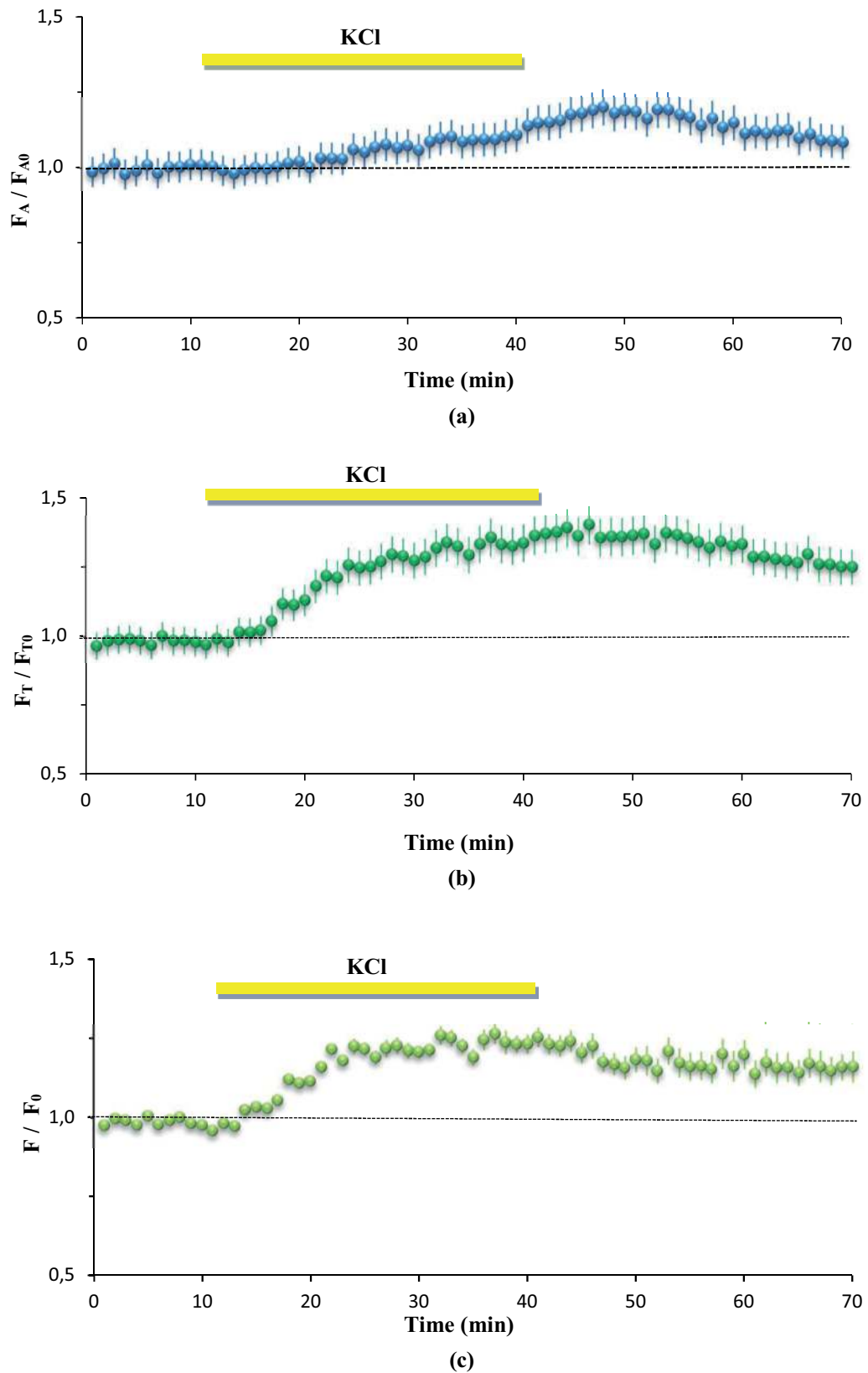


Figure 1. Autofluorescence, total fluorescence and zinc signals evoked by KCl. (a) KCl-induced changes in autofluorescence ($n = 4$). (b) Total fluorescence data obtained in slices incubated with NG ($n = 3$). (c) Zinc signals obtained as the difference between data in panels (b) and (a). The application of KCl (20 mM) was made at the times indicated by the bars. All values were normalized by the average of the first 10 responses and represent the mean \pm SEM. F_A , autofluorescence; F_T , total fluorescence; F , zinc signals; F_{A0} , F_{T0} , F_0 , basal auto-, total and zinc fluorescences, respectively.

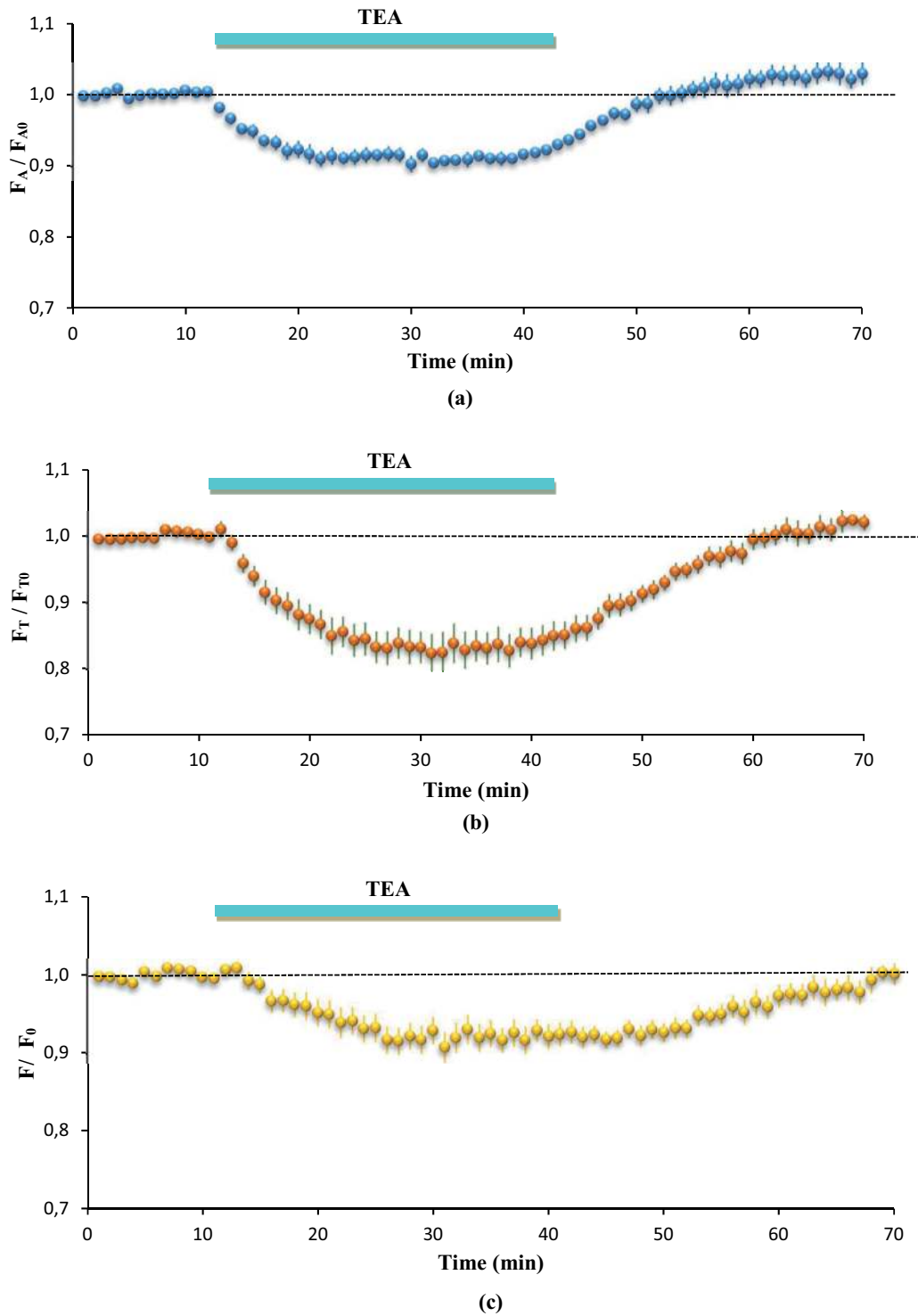


Figure 2. Pooled data of autofluorescence, total fluorescence and zinc signals evoked by TEA. (a) Effect of the application of TEA (25 mM) on autofluorescence changes ($n = 5$). (b) Total fluorescence signals obtained from slices incubated with NG ($n = 8$). (c) Zinc signals given by the difference between the traces in panels (a) and (b). The solution with TEA (25 mM) was perfused during the period indicated by the bars. All values were normalized by the average of the first 10 responses and represent the mean \pm SEM. F_A , autofluorescence; F_T total fluorescence; F , zinc signals; F_{A0} , F_{T0} , F_0 , basal auto-, total and zinc fluorescences, respectively.

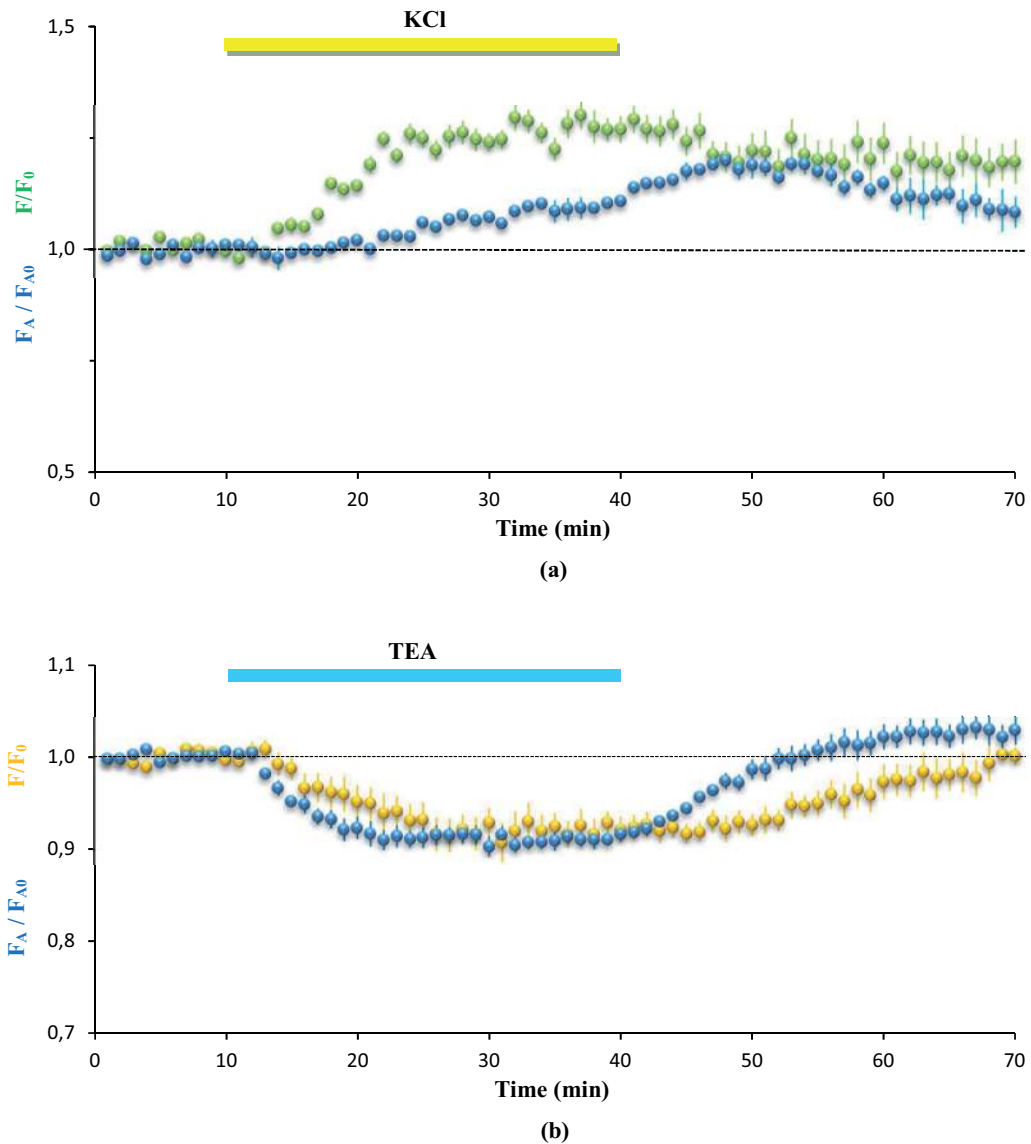


Figure 3. Superimposed curves of the KCl- and TEA-evoked fluorescence signals. (a) Autofluorescence (blue, $n = 3$) and zinc (green) signals induced by KCl (20 mM). (b) Autofluorescence (blue, $n = 5$) and zinc (orange) changes evoked by TEA (25 mM). The solutions of KCl and TEA were applied at the times indicated by the bars. All values were normalized by the average of the first 10 responses and represent the mean \pm SEM. F_A , autofluorescence; F , zinc fluorescence; F_{A0} , F_0 , basal auto- and zinc fluorescences.

In order to verify the involvement of K_{ATP} channels in the TEA induced fluorescence depression, tolbutamide, a K_{ATP} channel blocker was applied with TEA, at the concentrations of 250 μ M and 25 mM, respectively. In the control group of experiments, the TEA solution was perfused twice, circulating ACSF for 30 min after each TEA application, in order to determine the degree of recovery upon washout. In the other group of experiments, the second TEA solution contained also tolbutamide.

According to the results in **Figure 4**, both perfusions of the TEA solution caused similar declines in the intensity of the autofluorescence signals, which have also similar time courses as illustrated in **Figure 4a**. The first depression had an amplitude of $11 \pm 1\%$, with respect to baseline (35–40 min, $n = 3$). The second one had an

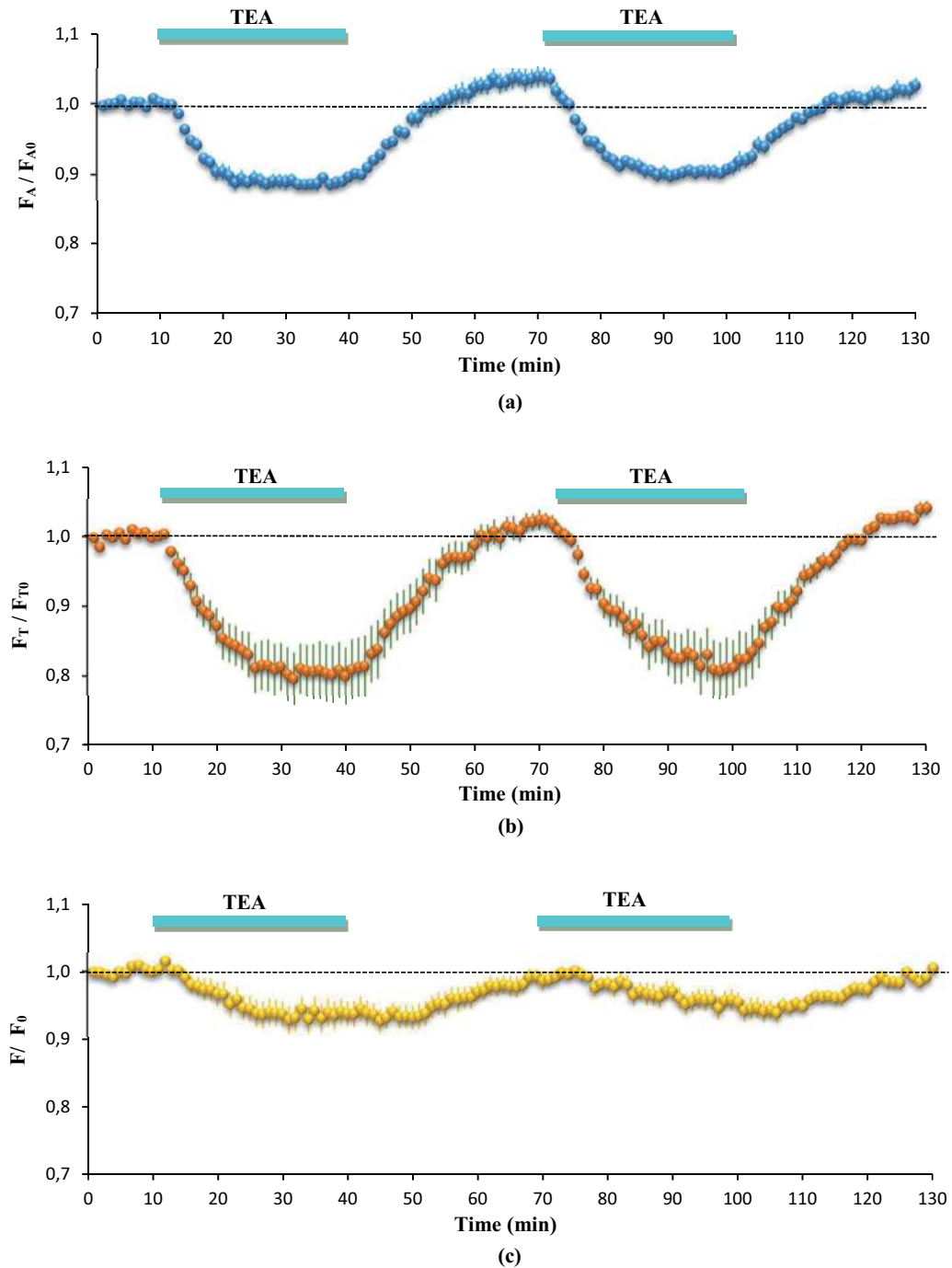


Figure 4. Fluorescence signals induced by two consecutive applications of TEA. (a) Autofluorescence responses ($n = 3$). (b) Total fluorescence data ($n = 8$). (c) Zinc signals calculated subtracting trace (a) from trace (b). The solution with TEA (25 mM) was circulated during the period indicated by the bars. All values were normalized by the average of the first 10 responses and are represented as mean \pm SEM. F_A , autofluorescence; F_T total fluorescence; F , zinc signals; F_{A0} , F_{T0} , F_0 , basal, auto-, total and zinc fluorescences, respectively.

amplitude of $10 \pm 2\%$ (95–100 min, $n = 3$). The washout of the TEA solution was, as expected, accompanied by the recovery of the autofluorescence signal, which reached, at the end of the subsequent 30 min period in ACSF, a small potentiation, $3 \pm 1\%$ at 65–70 min and $2 \pm 1\%$ at 125–130 min.

In a similar type of experiments, the second TEA application was combined with tolbutamide (250 μ M) (Figure 5). This compound had no effect on the

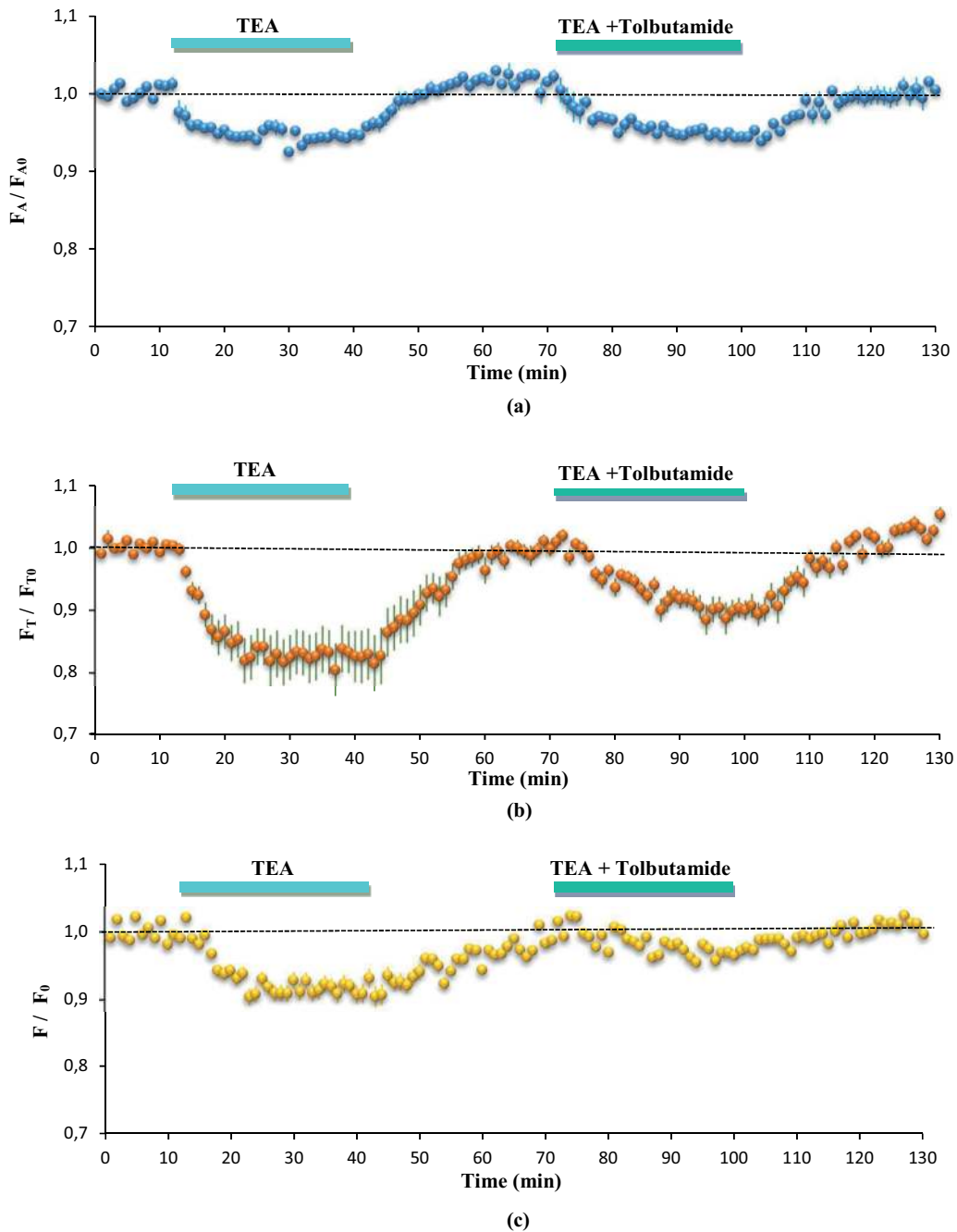


Figure 5. Tolbutamide significantly blocks zinc signals evoked by TEA. (a) Effect of the application of TEA (25 mM) followed by TEA (25 mM) plus tolbutamide (250 μ M) on autofluorescence ($n = 2$). (b) Similar records for total fluorescence ($n = 3$). (c) Zinc signals determined as trace (b) minus (a). The solutions of TEA and TEA plus tolbutamide were applied at the times indicated by the bars. The data were normalized by the average of the first 10 responses and represent the mean \pm SEM. F_A , autofluorescence; F_T , total fluorescence; F , zinc signals; F_{A0} , F_{T0} , F_0 , basal auto-, total and zinc fluorescences, respectively.

autofluorescence signal since the second depression was similar to the first one (**Figure 5a**), as observed in the experiment with two consecutive TEA applications (**Figure 4a**). On the other hand, the application of tolbutamide significantly blocked the depression of the total (**Figure 5b**) and of the zinc (**Figure 5c**) signals, having the latter been, once more, obtained subtracting the autofluorescence component from the total fluorescence changes. As noticed before, tolbutamide applied only in ACSF had essentially no effect on the autofluorescence depression.

The application of TEA evoked a depression of the zinc signal with an amplitude of $8 \pm 1\%$ (35–40 min, $n = 3$), while in the presence of tolbutamide, the corresponding amplitude was only $3 \pm 1\%$ (35–40 min, $n = 3$). Thus, tolbutamide blocks about two thirds of the TEA evoked zinc signal inhibition, suggesting that the zinc, but not the autofluorescence depression, is mainly mediated by the activation of K_{ATP} channels.

4. Discussion

The experiments presented in this work, performed at the hippocampal mossy fiber synapses from CA3 area, allow the comparison of autofluorescence signals, recorded from non-incubated slices, with fluorescence zinc changes obtained from NG-loaded slices, after subtraction of the autofluorescence component. At these synapses, it

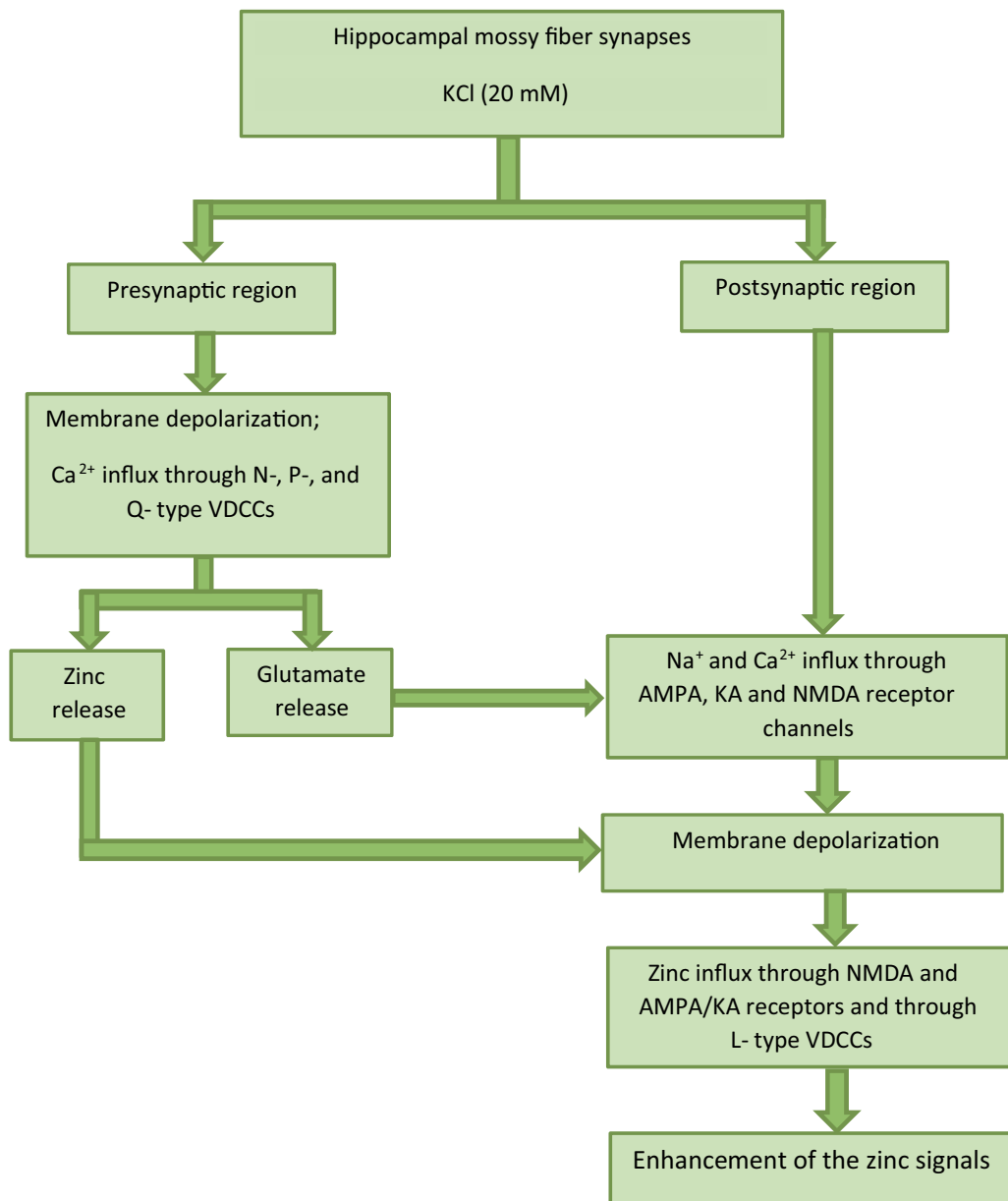


Figure 6. Schematic representation of the major cellular mechanisms and ionic fluxes involved in KCl depolarization (20 mM) at the hippocampal mossy fibers-CA3 pyramidal cells synapses.

was observed that chemically induced depolarization by KCl (20 mM), evoked clear autofluorescence changes that recovered partially during the 30 min period following washout. These changes have a lower amplitude and a slower time course than those of the similarly evoked fluorescence signals observed in slices incubated with the zinc indicator Newport Green. The latter signals, corresponding to the total fluorescence changes in this work, have previously been described by Bastos et al. [22]. The application of 20 mM KCl promotes the depolarization of the presynaptic membrane, mediated by voltage dependent potassium channels (VDKCs), to a resting value of about -54 mV [13]. This increase in the membrane potential activates presynaptic VDCCs, triggering glutamate and zinc co-release, as illustrated in **Figure 6**.

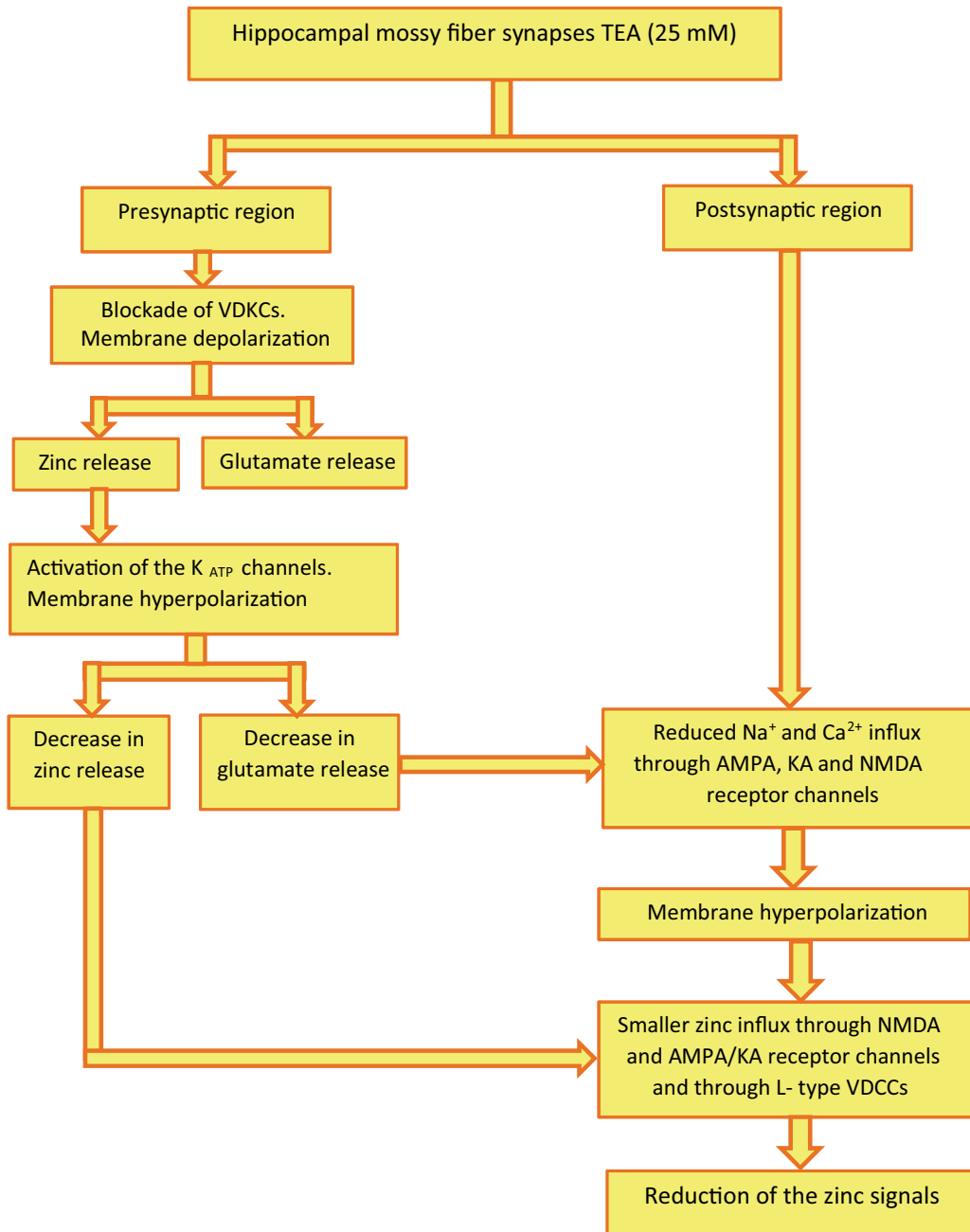


Figure 7. Diagram of the principal mechanisms and ionic movements involved in TEA depolarization at the hippocampal mossy fiber-CA₃ synaptic system.

Subsequently, after diffusion in the cleft and binding to specific pre- and postsynaptic sites, zinc flows into the postsynaptic region through several channels and receptors, including NMDA and calcium permeable AMPA/KA receptors and L- and T-type VDCCs [3–5, 8, 34]. There is also experimental evidence that zinc can be released from intracellular sources following blockade of ERs [35, 36]. Consequently, at the postsynaptic region, calcium and zinc entry through both glutamate receptor channels and VDCCs leads to cytosolic calcium and zinc accumulation that may cause the flow of both ions to mitochondria, through the activation of the mitochondrial Ca-uniporter [30, 37–43].

TEA also causes membrane depolarization that may trigger various cellular processes, as described in **Figure 7**.

In this work, the autofluorescence changes evoked by a single or by consecutive identical TEA applications were all similar. Interestingly, the time course of these changes is similar to that of the corresponding fluorescence signals recorded from Newport Green loaded slices. The TEA triggered fluorescence changes are depressed during the perfusion of TEA and recover to or above the baseline level upon washout, as previously reported [24]. In the present study, after subtracting the autofluorescence component, the real zinc signals evoked by TEA have about half the amplitude of that of the total fluorescence traces.

The changes of both autofluorescence and total fluorescence TEA induced signals are the opposite of those evoked by KCl. As previously mentioned, the membrane depolarization is higher in the presence of KCl than in TEA. The blockade of presynaptic VDCCs by TEA evokes a weak depolarization [23], followed by glutamate and zinc release and the activation of K_{ATP} channels by this ion. This leads to membrane hyperpolarization with a lower amplitude than that of the KCl evoked depolarization. Consequently, the hyperpolarizing effect of the zinc induced activation of presynaptic K_{ATP} channels can be occulted by the large increase in the resting potential, due to the strong KCl evoked depolarization, mediated by VDCCs [13].

5. Conclusions

The amount of calcium entry is related to the intensity of autofluorescence because increased intracellular calcium and zinc can trigger an increase in FAD (flavoprotein) and NAD, as well as in the oxidation of $FADH_2$ and NADH [28, 44]. In the present experimental conditions (excitation wavelength of 480 nm, emission light collected above 500 nm) and taking into account the spectral properties of FAD, the autofluorescence detected is considered to have FAD origin. As previously mentioned, KCl depolarization causes the entry of both calcium and zinc ions to the postsynaptic region [10, 22, 24, 45, 46]. When increases in cytosolic zinc concentration are high, zinc ions enter the mitochondria, and if in excess may have neurotoxic effects [4, 47, 48]. Thus, the origin of the KCl evoked autofluorescence signals is, under our experimental conditions and based on previous studies, the flavoproteins. For example, Pancani [49], have found, using the complex I inhibitor rotenone a KCl induced NADH fluorescence decrease of mitochondrial origin. This is in agreement with the observed FAD enhancement since the NADH and FAD fluorescence changes are opposite [29, 44, 50].

Acknowledgements

We thank CNC - Center for Neuroscience and Cell Biology, University of Coimbra, Coimbra, Portugal, for providing the rat brains. Work funded by strategic

project UID/NEU/04539/2013. All authors are aware of and have approved the manuscript as submitted. All authors are aware they must each submit a completed License to Publish form before the manuscript can be published. (Each author will receive an email with instructions).

Author details

Fatima M.C. Bastos^{1,2}, Carlos M. Matias^{1,3*}, Ines O. Lopes², João P. Vieira⁴, Rosa M. Santos^{1,4}, Luis M. Rosario^{1,4}, Rosa M. Quinta-Ferreira⁵ and Maria Emilia Quinta-Ferreira^{1,2}

1 CNC, University of Coimbra, Coimbra, Portugal

2 Department of Physics, University of Coimbra, Coimbra, Portugal

3 Department of Physics, School of Science and Technology, UTAD, Vila Real, Portugal

4 Department of Life Sciences, University of Coimbra, Coimbra, Portugal

5 CIEPQPF-Department of Chemical Engineering, University of Coimbra, Coimbra, Portugal

*Address all correspondence to: cmatias@utad.pt

IntechOpen

© 2021 The Author(s). Licensee IntechOpen. This chapter is distributed under the terms of the Creative Commons Attribution License (<http://creativecommons.org/licenses/by/3.0>), which permits unrestricted use, distribution, and reproduction in any medium, provided the original work is properly cited. 

References

- [1] Vallee, B.L. and Falchuk, K.H. (1993). The biochemical basis of zinc physiology. *Physiol. Rev.* 73: 79-118. <https://doi.org/10.1152/physrev.1993.73.1.7> PMID: 8419966.
- [2] Frederickson C.J., Suh S.W., Silva D., Frederickson C.J. and Thompson R.B. (2000). Importance of zinc in the central nervous system: The zinc-containing neuron. *J. Nutr.* 130: 1471S-1483S. <https://doi.org/10.1093/jn/130.51471S> PMID: 10801962.
- [3] Sensi S.L., Canzoniero L.M.T., Yu S.P., Ying H.S., Koh J.-Y., Kerchner G.A. and Choi D.W. (1997). Measurement of intracellular free zinc in living cortical neurons, routes of entry. *J. Neurosci.* 17: 9554-9564. <https://doi.org/10.1523/JNEUROSCI.17-24-09554.1997> PMID: 9391010.
- [4] Sensi S.L., Yin H.Z., Carriedo S.G., Rao S.S. and Weiss J.H. (1999). Preferential Zn²⁺ influx through Ca²⁺-permeable AMPA/kainate channels triggers prolonged mitochondrial superoxide production. *Proc. Natl. Acad. Sci. USA.* 96: 2414-2419. <https://doi.org/10.1073/pnas.96.5.2414> PMID: 10051656.
- [5] Marin, P., Israël, M., Glowinski, J. and Prémont, J. (2000). Route of zinc entry in mouse cortical neurons, role in zinc-induced neurotoxicity. *Eur. J. Neurosci.* 12: 8-18. <https://doi.org/10.1046/j.1460-9568.2000.00875.x> PMID: 10651855.
- [6] Dietz, R.M., Weiss, J.H. and Shuttleworth, C.W. (2008). Zn²⁺ influx is critical for some forms of spreading depression in brain slices. *J. Neurosci.* 28: 8014-8024. <https://doi.org/10.1523/JNEUROSCI.0765-08.2008> PMID: 18685026.
- [7] Quinta-Ferreira, M.E., Sampaio dos Aidos, F.D.S., Matias, C.M., Mendes, P.J., Dionísio, J.C., Santos, R.M., Rosário, L.M. and Quinta-Ferreira, R.M. (2016). Modelling zinc changes at the hippocampal mossy fiber synaptic cleft. *J. Comput. Neurosci.* 41, 323-337 (2016). <https://doi.org/10.1007/s10827-016-0620-x>.
- [8] Freitas, J.C.S, Miraldo, J.N., Matias, C., Sampaio Dos Aidos, F.D.S., Mendes, P.J., Dionísio, J.C., Santos, R.M., Rosário, L.M., Quinta-Ferreira, R.M. and Quinta-Ferreira M.E. (2019). Computer Simulations of Hippocampal Mossy Fiber Cleft Zinc Movements. *Advances in Neural Signal Processing* (ISBN 978-1-78984-114-5).
- [9] Vogt, K., Mellor, J., Tong, G. and Nicoll, R. (2000). The actions of synaptically released zinc at hippocampal mossy fiber synapses. *Neuron.* 26: 187-196. [https://doi.org/10.1016/S0896-6273\(00\)81149-6](https://doi.org/10.1016/S0896-6273(00)81149-6).
- [10] Li, Y., Hough, C.J., Frederickson, C.J. and Sarvey, J.M. (2001b). Rapid translocation of Zn²⁺ from presynaptic terminals into postsynaptic hippocampal neurons after physiological stimulation. *J. Neurophysiol.* 86: 2597-2604. <https://doi.org/10.1152/jn.2001.86.5.2597> PMID: 11698545.
- [11] Quinta-Ferreira, M.E. and Matias, C.M. (2005). Tetanically released zinc inhibits hippocampal mossy fiber calcium, zinc and postsynaptic responses. *Brain Res.* 1047: 1-9. <https://doi.org/10.1016/j.brainres.2005.04.006> PMID: 15950598.
- [12] Takeda A., Fuke S., Tsutsumi W. and Oku N. (2007). Negative modulation of presynaptic activity by zinc released from Schaffer collaterals. *J. Neurosci. Res.* 85: 3666-3672. <https://doi.org/10.1002/jnr.21449> PMID: 17680671.
- [13] Bancila, V., Nikonenko, I., Dunant, Y. and Bloc, A. (2004). Zinc inhibits

glutamate release via activation of pre-synaptic KATP channels and reduces ischaemic damage in rat hippocampus. *J. Neurochem.* 90: 1243-1250 <https://doi.org/10.1111/j.1471-4159.2004.02587.x>. PMID: 15312179.

[14] Matias, C.M., Saggau, P. and Quinta-Ferreira, M.E. (2010). Blockade of presynaptic KATP channels reduces the zinc-mediated posttetanic depression at hippocampal mossy fiber synapses. *Brain Res.* 1320: 22-27. <https://doi.org/10.1016/j.brainres.2010.01.021> PMID: 20097182.

[15] Büsselberg, D., Michael, D., Evans, M.L., Carpenter, D.O. and Haas, H.L. (1992). Zinc (Zn²⁺) blocks voltage gated calcium channels in cultured rat dorsal root ganglion cells. *Brain Res.* 593: 77-81. [http://doi.org/10.1016/0006-8993\(92\)91266-H](http://doi.org/10.1016/0006-8993(92)91266-H) PMID: 1333873.

[16] Harrison, N.L. and Gibbons, S.J. (1994). Zn²⁺: an endogenous modulator of ligand- and voltage-gated ion channels. *Neuropharmacology.* 33: 935-952. [http://doi.org/10.1016/0028-3908\(94\)90152-x](http://doi.org/10.1016/0028-3908(94)90152-x) PMID: 7845550.

[17] Assaf, S.Y. and Chung, S.H. (1984). Release of endogenous Zn²⁺ from brain tissue during activity. *Nature.* 308: 734-736. <https://doi.org/10.1006/exnr.1998.6931> PMID: 6717566.

[18] Budde, T., Minta, A., White, J. A. and Kay, A.R. (1997). Imaging free zinc in synaptic terminals in live hippocampal slices. *Neurosci.* 79: 347-358. [https://doi.org/10.1016/S0306-4522\(96\)00695-1](https://doi.org/10.1016/S0306-4522(96)00695-1) PMID: 9200720.

[19] Quinta-Ferreira, M.E., Matias, C.M., Arif, M. and Dionísio, J.C. (2004). Measurement of presynaptic zinc changes in hippocampal mossy fibers. *Brain Res.* 1026: 1-10. <https://doi.org/10.1016/j.brainres.2004.07.054>. PMID: 15476692.

[20] Bernard, J., Lahsaini, A. and Massicotte, G. (1994). Potassium-induced long-term potentiation in area CA1 of the hippocampus involves phospholipase activation. *Hippocampus.* 4: 447-453. <https://doi.org/10.1002/hipo.450040407> PMID: 7874236.

[21] Roisin, M.-P., Leinekugel, X. and Tremblay, E. (1997). Implication of protein kinase C in mechanisms of potassium-induced long-term potentiation in rat hippocampal slices. *Brain Res.* 745: 222-230. [https://doi.org/10.1016/S0006-8993\(96\)01155-9](https://doi.org/10.1016/S0006-8993(96)01155-9).

[22] Bastos, F.M.C., Lopes, S.A., Corceiro, V.N., Matias, C.M., Dionísio, J.C., Aidos, F.D.S.S., Mendes P.J., Santos, R.M., Quinta-Ferreira, R.M. and Quinta-Ferreira, M.E. (2017a). Postsynaptic zinc potentiation elicited by KCl depolarization at hippocampal mossy fiber synapses. *Gen. Physiol. Biophys.* 36: 289-296. https://doi.org/10.4149/gpb_2017001 PMID: 28471347.

[23] Song, D., Wang, Z. and Berge, T.W. (2002). Contribution of T-Type VDCC to TEA-Induced Long-Term Synaptic Modification in Hippocampal CA1 and Dentate Gyrus. *Hippocampus* 12: 689 – 697. DOI 10.1002/hipo.10105.

[24] Bastos, F.M., Corceiro, V.N., Lopes, S.A., Almeida, J.G., Matias, C.M., Dionísio, J.C., Mendes, P.J., Sampaio dos Aidos, F.D.S., Quinta-Ferreira, R.M. and Quinta-Ferreira, M.E (2017b). Effect of tolbutamide on tetraethylammonium-induced postsynaptic zinc signals at hippocampal mossy fiber-CA3 synapses. *Can. J. Physiol. Pharmacol.* 95 (9): 1058-1063. <https://doi.org/10.1139/cjpp-2016-0379> PMID: 28654763.

[25] Bossy-Wetzel, E., Talantova, M.V., Lee, W.D., Scholzke, M.N., Harrop, A., Mathews, E., Gotz, T., Han, J., Ellisman, M.H., Perkins, G.A. and Lipton, S.A. (2004). Crosstalk between nitric oxide

and zinc pathways to neuronal cell death involving mitochondrial dysfunction and p38-activated K⁺ channels. *Neuron*. 41: 351-365. PMID: 14766175.

[26] Medvedeva, Y.V., Lin, B., Shuttleworth, C.W. and Weiss, J.H. (2009). Intracellular Zn²⁺ accumulation contributes to synaptic failure, mitochondrial depolarization, and cell death in an acute slice oxygen-glucose deprivation model of ischemia. *J Neurosci*. 29: 1105-1114. <https://doi.org/10.1523/JNEUROSCI.4604-08.2009> PMID: 19176819.

[27] Reinert, K.C., Dunbar, R.L., Gao, W., Chen, G. and Ebner, T.J. (2004). Flavoprotein autofluorescence imaging of neuronal activation in the cerebellar cortex in vivo. *J. Neurophysiol.* 92(1), 199-211. <https://doi.org/10.1152/jn.01275.2003> PMID: 14985415.

[28] Brennan, A.M., Connor, J.A. and Shuttleworth, C.W. (2006). NAD(P)H Fluorescence Transients after Synaptic Activity in Brain Slices: Predominant Role of Mitochondria Function. *J. Cereb. Blood Flow Metab.* 26: 1389-1406. <https://doi.org/10.1038/sj.jcbfm.9600292>.

[29] Shuttleworth, C.W. (2010). Use of NAD(P)H and Flavoprotein Autofluorescence Transients to Probe Neuron and Astrocyte Responses to Synaptic Activation. *Neurochem. Int.* 56: 379-386. <https://doi.org/10.1016/j.neuint.2009.12.015> PMID: 20036704.

[30] Sensi, S. L., Ton-That, D., Sullivan, P.G., Jonas, E.A., Gee, K.R., Kaczmarek, L.K. and Weiss, J.H. (2003). Modulation of mitochondrial function by endogenous Zn²⁺ pools. *PNAS*. 10: 6157-6162. <http://doi.org/10.1073/pnas.1031598100> PMID: 12724524.

[31] Sensi, S.L., Paoletti, P., Bush, A.I. and Sekler, I. (2009). Zinc in the physiology and pathology of the CNS. *Nat Rev Neurosci*. 10(11): 780-91.

<https://doi.org/10.1038/nrn2734> PMID: 19826435.

[32] Shuttleworth, C.W. and Weiss, J.H. (2011). Zinc: new clues to diverse roles in brain ischemia. *Trends Pharmacol. Sci.* 32: 480-486. <https://doi.org/10.1016/j.tips.2011.04.001> PMID: 21621864.

[33] Denton, R.M. (2009). Regulation of mitochondrial dehydrogenases by calcium ions. *Biochem. Biophys. Acta.* 1787: 1309-1326. <https://doi.org/10.1016/j.bbabi.2009.01.005> PMID: 19413950.

[34] Takeda, A., Sakurada, N., Ando, M., Kanno, S. and Oku, N. (2009). Facilitation of zinc influx via AMPA/kainate receptor activation in the Hippocampus. *Neurochem. Intl.* 55: 376-382. <https://doi.org/10.1016/j.neuint.2009.04.006>.

[35] Stork, C. and Li, Y. (2010). Zinc release from thapsigargin/IP3- sensitive stores in cultured cortical neurons. *J. Mol. Signaling.* 5: 1-6. <https://doi.org/10.1186/1750-2187-5-5>.

[36] McCord, M. and Aizenman, E. (2014). The role of intracellular zinc release in aging, oxidative stress, and Alzheimer's disease. *Front Aging Neurosci.* 6: 77 (1-16). <https://doi.org/10.3389/fnagi.2014.00077>.

[37] Jiang, D., Sullivan, P.G., Sensi, S.L., Steward, O. and Weiss, J.H. (2001). Zn(2+) induces permeability transition pore opening and release of pro-apoptotic peptides from neuronal mitochondria. *J. Biol. Chem.* 276:47524-47529. <https://doi.org/10.1074/jbc.M108834200>.

[38] Dineley, K.E., Malaiyandi, L.M. and Reynolds, I.J. (2002). A reevaluation of neuronal zinc measurements: artifacts associated with high intracellular dye concentration. *Mol. Pharmacol.* 62: 618-627. <https://doi.org/10.1124/mol.62.3.618> PMID: 12181438.

- [39] Dineley, K.E., Votyakova, TV. and Reynolds, I.J. (2003). Zinc inhibition of cellular energy production: implications for mitochondria and neurodegeneration. *J. Neurochem.* 85: 563-70. <https://doi.org/10.1046/j.1471-4159.2003.01678.x> PMID: 12694382.
- [40] Gazaryan, I.G., Krasinskaya, I.P., Kristal, B.S. and Brown. A.M. (2007). Zinc irreversibly damages major enzymes of energy production and antioxidant defense prior to mitochondrial permeability transition. *J. Biol. Chem.* 282: 24373-24380. [https://doi.org/ DOI 10.1074/jbc.M611376200](https://doi.org/DOI%2010.1074/jbc.M611376200).
- [41] Sindreu C, Storm D.R. (2011). Modulation of neuronal signal transduction and memory formation by synaptic zinc. *Front Behav Neurosci.* 5: 68. <https://doi.org/10.3389/fnbeh.2011.00068> PMID: 22084630.
- [42] Quan, X., Thi-Nguyen, T., Choi, S.-K., Xu, S., Das, R., Cha, S.-K., Kim, N., Han, J., Wiederkehr, A., Wollheim, C.B and Park, K-S. (2015). Essential Role of Mitochondrial Ca²⁺ Uniporter in the Generation of Mitochondrial pH Gradient and Metabolism-Secretion Coupling in Insulin-releasing Cells. *J. Biol. Chem.* 290, 4086-4096. DOI :<https://doi.org/10.1074/jbc.M114.632547>.
- [43] Oropeza-Almazan, Y. and Blater, L.A. (2020). Mitochondrial calcium uniporter complex activation protects against calcium alternans in atrial myocytes. *American Journal of Physiology-Heart and Circulatory Physiology*, 319, 4. <https://doi.org/10.1152/ajpheart.00375.2020>.
- [44] Bartolomé, F. and Abramov, A. Y. (2015). Measurement of Mitochondrial NADH and FADAutofluorescence in Live Cells. *Metho. Mol. Bio.* 1264:263-0. doi.org/10.1007/978-1-4939-2257-4_23.
- [45] Colvin, R.A., Fontaine, C.P., Laskowski, M. and Thomas, D. (2003). Zn²⁺ transporters and Zn²⁺ homeostasis in neurons. *Eur. J. Pharmacol.* 479(1-3): 171-185. [https://doi.org/ 10.1016/j.ejphar.2003.08.067](https://doi.org/10.1016/j.ejphar.2003.08.067) PMID: 14612148.
- [46] Li, Y., Hough, C.J., Suh, S.W., Sarvey, J.M. and Frederickson, C.J. (2001a). Induction of mossy fiber, CA3 long-term potentiation requires translocation of synaptically released Zn²⁺. *J. Neurosci.* 21: 8015-8025. [https://doi.org/270-6474/01/218015-11\\$15.00/0](https://doi.org/270-6474/01/218015-11$15.00/0) PMID: 11588174.
- [47] Choi, D.W. and Koh, J.Y. (1998). Zinc and brain injury. *Ann. Rev. Neurosci.* 21: 347-375. <https://doi.org/10.1146/annurev.neuro.21.1.347> PMID: 9530500.
- [48] Galasso, S.L. and Dyck, R.H. (2007). The role of zinc in cerebral ischemia. *Mol. Med.* 13: 380-387. <https://doi.org/10.2119/2007-00044.Galasso> PMID: 17622314.
- [49] Pancani, T., Anderson, K.L., Porter, N.M., and Thibault, O. (2011). Imaging of a glucose analog, calcium and NADH in neurons and astrocytes: dynamic responses to depolarization and sensitivity to pioglitazone. *Cell Calcium.* 50: 548-558. doi.org/10.1016/j.ceca.2011.09.002. PMID: 21978418.
- [50] Kosterin, P., Kim, G.H., Muschol, M., Obaid, A.L. and Salzberg, B.M. (2005). Changes in FAD and NADH Fluorescence in Neurosecretory Terminals Are Triggered by Calcium Entry and by ADP Production. *J. Membr. Biol.* 208(2): 113-124. <https://doi.org/10.1007/s00232-005-0824-x> PMID: 16645741.